AAPS PharmSciTech, Vol. 13, No. 4, December 2012 (© 2012)
DOI: 10.1208/s12249-012-9866-4

Research Article

Formation of Itraconazole–Succinic Acid Cocrystals by Gas Antisolvent Cocrystallization

Courtney A. Ober[1,2] and Ram B. Gupta[1]

Received 5 June 2012; accepted 25 September 2012; published online 9 October 2012

Abstract. Cocrystals of itraconazole, an antifungal drug with poor bioavailability, and succinic acid, a water-soluble dicarboxylic acid, were formed by gas antisolvent (GAS) cocrystallization using pressurized CO_2 to improve itraconazole dissolution. In this study, itraconazole and succinic acid were simultaneously dissolved in a liquid solvent, tetrahydrofuran, at ambient conditions. The solution was then pressurized with CO_2, which decreased the solvating power of tetrahydrofuran and caused crystallization of itraconazole–succinic acid cocrystals. The cocrystals prepared by GAS cocrystallization were compared to those produced using a traditional liquid antisolvent, *n*-heptane, for crystallinity, chemical structure, thermal behavior, size and surface morphology, potential clinical relevance, and stability. Powder X-ray diffraction, Fourier transform infrared spectroscopy, differential scanning calorimetry, and scanning electron microscopy analyses showed that itraconazole–succinic acid cocrystals with physical and chemical properties similar to cocrystals produced using a traditional liquid antisolvent technique can be prepared by CO_2 antisolvent cocrystallization. The dissolution profile of itraconazole was significantly enhanced through GAS cocrystallization with succinic acid, achieving over 90% dissolution in less than 2 h. The cocrystals appeared stable against thermal stress for up to 4 weeks under accelerated stability conditions, showing only moderate decreases in their degree of crystallinity but no change in their crystalline structure. This study shows the utility of an itraconazole–succinic acid cocrystal for improving itraconazole bioavailability while also demonstrating the potential for CO_2 to replace traditional liquid antisolvents in cocrystal preparation, thus making cocrystal production more environmentally benign and scale-up more feasible.

KEY WORDS: cocrystals; dissolution rate; gas antisolvent; itraconazole.

INTRODUCTION

Control over the solid-state form of an active pharmaceutical ingredient (API) can provide opportunities for engineering desirable physical and clinically relevant API properties. Cocrystals, or stoichiometric multi-component crystalline solids, have recently emerged as a versatile tool offering numerous advantages for pharmaceutical formulation. By judicious selection of an appropriate former molecule, pharmaceutical cocrystals can enhance API solubility (1,2), stability (3), and mechanical properties (4,5). The commercial adoption of pharmaceutical cocrystalline forms will rely on the development of scalable, environmentally benign processes capable of producing sufficient quantities of cocrystals which conform to the existing standards of purity and reproducibility. Traditional cocrystal production has been accomplished by grinding, neat or solvent-facilitated (6,7), or solution-based methods which induce supersaturation by cooling, solvent evaporation, or the addition of a liquid antisolvent (8,9). The mechanical stress invoked during grinding and associated heat evolution can affect the stability of certain APIs while the large amounts of organic solvent used in solution-based methods are environmentally undesirable. Recently, supercritical CO_2-based processes, which minimize organic solvent use, have also been used for cocrystal production (10,11). Supercritical CO_2 is a favorable reaction medium since it is nontoxic, nonflammable, inexpensive, and has a relatively low critical temperature and critical pressure (T_c=31.1°C, P_c=73.8 bar) (12).

The low solubility of many pharmaceutical compounds in supercritical CO_2 makes CO_2 antisolvent techniques ideal for crystallization. Two of the most common CO_2 antisolvent techniques for the crystallization of pharmaceuticals are supercritical antisolvent (SAS) and gas antisolvent (GAS). In the SAS technique, a solute-containing solution is sprayed through a nozzle into a high-pressure vessel containing supercritical CO_2. The organic solvent diffuses into the CO_2 while the CO_2 also diffuses into the organic phase, inducing supersaturation and causing solute crystallization. Padrela *et al.* previously used the SAS process to form indomethacin–saccharin cocrystals (10). In the GAS technique, compressed CO_2 is added to a solute-containing solution in a high-pressure vessel. The CO_2 dissolves into the liquid solvent, causing the liquid solvent to expand, its solubilizing power to decrease, and the solute to crystallize. GAS crystallization has been used extensively for the pharmaceutical tailoring

[1] Department of Chemical Engineering, Auburn University, 212 Ross Hall, Auburn, Alabama 36849, USA.
[2] To whom correspondence should be addressed. (e-mail: CourtneyOber@gmail.com)

of pure component properties for APIs including phenanthrene (13), sulfathiazole (14), hydrocortisone (15), griseofulvin (16), and theophylline (17).

Incorporation of multiple solutes in GAS crystallization has focused on fractionation, composite production, and very limitedly, crystal growth manipulation. Starting from an equimolar solution of phenanthrene and naphthalene in toluene, greater than 98.5% pure phenanthrene could be crystallized by CO_2 pressurization while naphthalene with 13% phenanthrene was collected from the liquid phase following expansion (18). Drug–polymer composites, including hydrocortisone–polyvinylpyrrolidone (PVP), insulin–polyethylene glycol (PEG), and insulin–poly L-lactide (PLA), have been developed for controlled release formulations by co-precipitation using the GAS technique (15,19). The crystal growth orientation preference of caffeine could be manipulated by addition of α-D-glucose penta acetate, a growth retardant, during GAS recrystallization (20). To the best of our knowledge, carbamazepine–nicotinamide cocrystals were the first to be formed using GAS crystallization, but the focus of this study was on the cocrystals' complexation with γ-cyclodextrin, not cocrystal formation (21). A prior work from our laboratory was the first to systematically study the formation of cocrystals using GAS crystallization (22). In this study, itraconazole/L-malic acid cocrystals, along with some unquantified amount of amorphous material, were precipitated from tetrahydrofuran using pressurized CO_2. The itraconazole/L-malic acid cocrystals had a low degree of crystallinity, but exhibited slightly improved dissolution over the pure drug.

A number of unique advantages and opportunities exist when using GAS cocrystallization for pharmaceutical cocrystal engineering. GAS cocrystallization reduces thermal and mechanical stress on the API compared to grinding processes, reduces organic solvent use compared to traditional solution-based processes in favor of environmentally benign CO_2, and allows facile recycling of the original organic solvent by simple depressurization. In addition, the molecular recognition events that occur during cocrystal formation are influenced by and can be manipulated with the environment in which they are occurring. For example, the use of a supercritical enhanced atomization process generated a novel theophylline—saccharin cocrystal previously undiscovered through a thermal cocrystal screening method (11,23). Furthermore, the influence of operating conditions in CO_2 antisolvent processes on the crystal structure of recrystallized APIs has been well documented (17,24–28). GAS recrystallization of beclomethasone-17,21-dipropionate from acetone gave a more crystalline product, as indicated by increased peak intensities in the X-ray diffraction (XRD) pattern, compared to GAS recrystallization from methanol or ethanol (28). Recrystallization of theophylline using both the GAS and SAS techniques resulted in changes in the crystal lattice of the drug, as evidenced by new peaks in the XRD patterns (17). These few examples illustrate the crystal engineering flexibility of GAS crystallization and justify further exploration into its potential in developing pharmaceutical cocrystals. In this study, an itraconazole–succinic acid cocrystal previously prepared by a solution-based method was prepared by GAS cocrystallization using CO_2 as the antisolvent. The itraconazole–succinic acid cocrystal was selected for development on the basis of its existing crystal structure characterization and demonstrated bioavailability improvement (29).

MATERIALS AND METHODS

Materials

Micronized itraconazole was purchased from Hawkins Pharmaceutical Group (Minneapolis, MN). Succinic acid was purchased from Sigma Aldrich (St. Louis, MO). ACS-grade tetrahydrofuran (THF) and HPLC-grade *n*-heptane were purchased from Mallinckrodt Chemicals (Phillipsburg, NJ) and Fisher Scientific (Fair Lawn, NJ), respectively. Bone-dry carbon dioxide was purchased from Airgas (Opelika, AL). All other chemicals were reagent grade and used as received.

Cocrystallization by Liquid Antisolvent

Itraconazole (250 mg) and succinic acid (100 mg) were dissolved in 10 mL of THF using moderate stirring and heat. The solution was then filtered through a 0.2-μm pore size nylon filter (Whatman, Inc., Florham Park, NJ) to remove any undissolved material. *N*-heptane (20 mL) was then added dropwise to the solution, with continuous stirring, to induce cocrystallization. The suspension was centrifuged and the supernatant removed. The cocrystals were then washed with additional *n*-heptane and the centrifugation and supernatant removal process carried out an additional three times to ensure full removal of the THF. The cocrystals were allowed to dry overnight.

Gas Antisolvent Cocrystallization

A schematic of the GAS cocrystallization apparatus is shown in Fig. 1. The 37-mL stainless steel crystallization vessel (Thar Technologies, Inc., Pittsburgh, PA) is equipped with multiple sapphire windows for observation. A 0.2-μm filter was attached to the CO_2 inlet line within the crystallization vessel which allowed CO_2 to be sparged through the liquid solution, thus enhancing mass transfer. A second stainless steel vessel was connected in series prior to the crystallization vessel to moderate CO_2 pressurization by acting as a CO_2 reservoir. The pressure inside each vessel was measured using a 0–345±1.7-bar pressure gauge. The temperature inside both vessels was maintained at 40±2°C using a standard thermocouple and heating tape. The outlet line to valve V3 contained a 0.5-μm stainless steel frit to prevent loss of powder during flushing.

Itraconazole (250 mg) and succinic acid (100 mg) were dissolved in 10 mL of THF using moderate stirring and heat. The solution was then filtered through a 0.2-μm pore size nylon filter to remove any undissolved material and injected into the crystallization vessel. With valves V2 and V3 closed, compressed CO_2 was chilled, pumped with a piston pump, and preheated to 40°C prior to entering the CO_2 reservoir. Upon filling the CO_2 reservoir to a sufficient pressure, valve V2 was slightly opened to allow a controlled flow of CO_2 into the crystallization vessel. Pressure was increased at a constant rate of approximately 4 bar/min over a period of 25 min until a final pressure of 103 bar was achieved. For solvent removal and CO_2 flushing, valve V3 was opened and a back pressure regulator was used to maintain the desired pressure (103 bar). Flushing with additional supercritical CO_2 was conducted for 60 min at a CO_2 flow rate of 5 g/min. The vessel was then

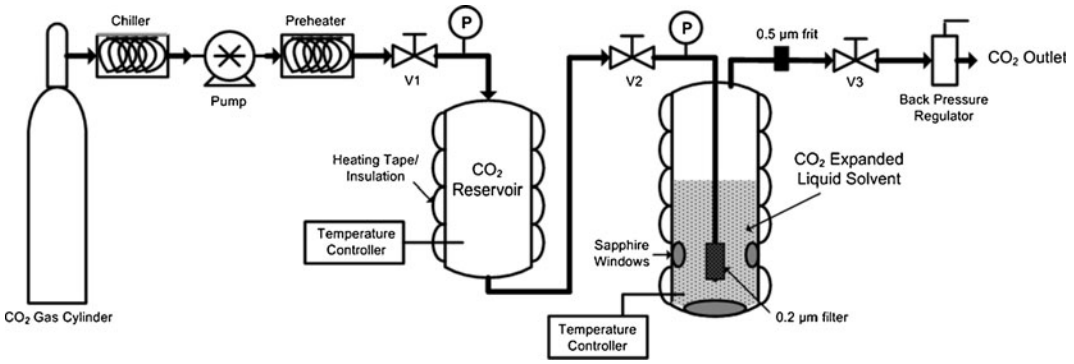

Fig. 1. Schematic of gas antisolvent cocrystallization apparatus

depressurized over a period of approximately 30 min and the cocrystals collected.

Powder X-Ray Diffraction

The crystallinity of the samples was assessed using a Bruker D8 Advance diffractometer equipped with a Co Kα radiation source operated at 40 kV and 40 mA except for the physical mixture whose powder X-ray diffraction (PXRD) pattern was collected at a later date using a Bruker D8 diffractometer equipped with a Cu Kα radiation source operated at 40 kV and 40 mA. A corundum standard (NIST SRM1976) was used for calibration (Co Kα 2θ=41.05°). Diffraction patterns were collected in the 2θ range of 5°–40° using a step size of 0.01° and a count time of 0.1 s/step. For comparison, the diffraction patterns found using Co Kα radiation (λ=1.790 Å) were converted to Cu Kα radiation diffraction patterns (λ=1.542 Å) and *vice versa* using the Bragg equation,

$$n\lambda = 2d\sin(\theta) \tag{1}$$

to calculate the d-spacing. However, all patterns shown in this work are on a cobalt basis.

The physical stability (shelf-life) of the cocrystal samples was evaluated by placing powder samples, contained in glass vials, in a 90°C/dry oven for 7, 14, and 28 days and assessing any changes in crystallinity by PXRD. All samples (including an untreated sample) were from the same batch and were analyzed at the same time, which allowed any changes in crystallinity to be attributed to thermal stress and not due to storage at ambient conditions.

Fourier Transform Infrared Spectroscopy

The infrared spectra were recorded on a Nicolet IR 100 (Thermo Scientific, USA). Each sample was mixed with 100-fold KBr for preparing the pellets. The final spectra consist of 128 scans performed in the range of 400–4,000 cm^{-1} with 4-cm^{-1} resolution.

Cocrystal Composition by High-Pressure Liquid Chromatography

Cocrystal composition was determined by dissolving a known concentration of cocrystals in methanol and analyzing the itraconazole content by high pressure liquid chromatography (HPLC). The relative standard deviation (RSD) of drug content for five samples was calculated from:

$$RSD = \frac{\sigma}{\overline{C}} \tag{2}$$

$$\sigma^2 = \frac{\sum_{i=1}^{n}\left(\overline{C} - C_i\right)^2}{n-1} \tag{3}$$

where n is the total number of samples, σ^2 is the variance, σ is the standard deviation, $\overline{C}$ is the mean concentration determined experimentally, and C_i is the sample concentration. A Waters (Milford, MA) HPLC system with a UV dual absorbance detector and Brownlee C18 column with inner diameter of 2.1 mm, length of 150 mm, particle size of 5 μm, and pore size of 100 Å manufactured by PerkinElmer (Waltham, MA) were used. A mobile phase of 0.01 M tetrabutylammonium hydrogen sulfate in water and acetonitrile (55:45% (*v*/*v*)) was pumped at a flow rate of 0.3 mL/min. Pressure was approximately 124 bar. Itraconazole content was assayed at λ=261 nm and a calibration curve was constructed using standards of 0.001–0.01 mg/mL in methanol.

Differential Scanning Calorimetry

Thermal behavior was studied using a Differential Scanning Calorimeter Autosampler System (TA Instruments, New Castle, DE). Approximately 5 mg of each sample was weighed in an aluminum pan and the thermographs recorded using a heating rate of 10°C/min under a nitrogen purge.

Scanning Electron Microscopy

Particle size and surface morphology were studied using a scanning electron microscope (Zeiss EVO 50, UK). Powder samples were sprinkled onto double-sided adhesive carbon tape on an aluminum stub. A thin coating (~15 nm) of gold was applied to the sample using an EMS 550X sputter coater (Hatfield, PA) prior to microscopy.

Dissolution Studies

Dissolution studies were performed in 450 mL of 0.1N HCl with 0.3% sodium dodecyl sulfate dissolution medium at 37±2°C. Stirring was accomplished by a four-blade radial flow

turbine operated at 50 rpm. Neat powders containing 5 mg of itraconazole, as calculated from the weight percent of itraconazole in the sample as determined by HPLC, were sprinkled onto the top of the dissolution medium. Liquid samples were withdrawn at time intervals of 5, 10, 15, 20, 30, 45, 60, 75, 90, and 120 min, filtered through 0.2-μm pore size nylon filters, and assayed for drug content by HPLC. Equivalent aliquots of dissolution medium were added following sample withdrawal to maintain constant volume. Dissolution studies were performed in duplicate for each sample. Dissolution profiles were constructed to show the amount of itraconazole dissolved as a function of time, with 5 mg of itraconazole representing 100% dissolution. Dissolution data are presented as the mean ± standard error.

RESULTS

Powder X-Ray Diffraction Patterns

The PXRD patterns for itraconazole, succinic acid, a 1:1 by mass physical mixture of the two, and the itraconazole—succinic acid cocrystals formed by liquid and CO_2 antisolvent techniques are shown in Fig. 2. Due to the intense crystalline nature of succinic acid, each pattern has been shown on its own scale, but the numerical intensities of each scale are equivalent. Itraconazole exhibited characteristic crystalline peaks at 2θ values of 17.0°, 20.6°, 21.1°, 23.9°, 27.6°, 29.8°, and 31.8°, in correspondence with the literature (30). Succinic acid exhibited characteristic crystalline peaks at 2θ values of 23.3°, 29.9°, 30.4°, 31.2°, and 36.9°, also in correspondence with the literature (31). The physical mixture exhibited crystalline peaks characteristic of both itraconazole and succinic acid. The itraconazole–succinic acid cocrystals exhibited intense crystalline peaks at 2θ values of 7.1°, 10.6°, 18.9°, 20.2°, 21.2°, 23.4°, 28.6°, and 31.1°.

Fourier Transform Infrared Spectra

Infrared spectroscopy was conducted to examine the nature of any interactions between itraconazole and succinic acid in the cocrystals. The Fourier transform infrared (FTIR) spectra for itraconazole, succinic acid, a 1:1 by mass physical mixture of the two, and the itraconazole–succinic cocrystals formed by liquid and CO_2 antisolvent techniques are shown in Fig. 3. The characteristic peaks of itraconazole occurred at 3,384, 3,126, 3,068, 2,962, 1,699, 1,510, and 1,450 cm^{-1}, in correspondence with the literature (32). The characteristic peaks of succinic acid occurred at 2,931, 2,650, 1,693, 1,417, 1,311, and 1,201 cm^{-1}, also in correspondence with the literature (33). Table I summarizes the vibrational frequencies of relevant hydrogen bonding functional groups in an itraconazole–succinic acid cocrystal. The O–H stretch of succinic acid occurred at 2,650 cm^{-1} for the pure former. The frequency of this stretch was decreased to 2,630 cm^{-1} in the itraconazole–succinic acid cocrystals prepared by each method. The C–N and C=N stretches in itraconazole occurred at 1,431 and 1,614 cm^{-1}, respectively, for the pure drug. The frequency of the C–N stretch for the cocrystals formed by both methods increased to 1,437 cm^{-1} while the frequency of the C=N stretch was unaffected (within the resolution limits of the scan).

Thermal Behavior

The thermal behavior of the pure components and cocrystals was studied by differential scanning calorimetry (DSC). The DSC thermographs for itraconazole, succinic acid, a 1:1 by mass physical mixture of the two, and the itraconazole–succinic acid cocrystals formed by liquid and CO_2 antisolvent are shown in Fig. 4. Itraconazole exhibited a well-defined melting endotherm at 169.4°C (ΔH_f=85.3 J/g). Succinic acid also showed a defined melting point at 191.3°C (ΔH_f=168.0 J/g), but underwent decomposition above 200°C. The physical mixture of itraconazole and succinic acid featured a melting endotherm at 151.3°C (ΔH_f= 50.8 J/g) and a broad endothermic event from 170°C to 185°C. The itraconazole–succinic acid cocrystals formed by liquid and CO_2 antisolvent techniques showed broad endothermic events between 145°C and 165°C.

Scanning Electron Microscopy Images

Scanning electron microscopy images of the pure components and cocrystals are shown in Fig. 5. Itraconazole, as obtained from the supplier, featured rod-like structures and smaller particles with average sizes ranging from 2 to 20 μm, as shown in Fig. 5a. Succinic acid, as obtained from the supplier, featured smooth semi-spherical particles with average sizes ranging from 50 μm to several hundred microns, as shown in Fig. 5b. The itraconazole–succinic acid cocrystals formed by the liquid antisolvent technique were thin flakey structures, as shown in Fig. 5c. Some of the flakes featured a hexagonal shape while others had less defined edges and a more irregular shape. Slow growth of itraconazole–succinic acid single cocrystals from 10/2/1 1,2-dichloro-ethane/ethyl acetate/1,4-dioxane solution also produced hexagonal plates (29). Spherical agglomerates of radiating plates were also evident. Cocrystallization using CO_2 as the antisolvent gave thin irregularly shaped flakes, as shown in Fig. 5d. Many of these flakes were oriented in rosette structures, with flattened radial agglomeration around a focal point.

Dissolution Profiles

Dissolution studies were conducted to assess the potential clinical relevance of an itraconazole–succinic acid cocrystal and to determine how the different methods of cocrystal preparation might affect clinically relevant drug properties such as dissolution rate. The dissolution profiles for itraconazole, a 1:1 by mass physical mixture of itraconazole and succinic acid, and the itraconazole–succinic acid cocrystals formed by liquid and CO_2 antisolvent are shown in Fig. 6. Itraconazole, despite being purchased in micronized form, exhibits poor dissolution achieving less than 30% release in 2 h. The dissolution profile of the physical mixture is nearly an upward linear shift of the pure itraconazole dissolution profile. This shift is likely caused by a decrease in itraconazole particle size from grinding the itraconazole and succinic acid together with a mortar and pestle to create the mixture. The itraconazole–succinic acid cocrystals prepared by both methods show significantly faster dissolution than the physical mixture, thereby demonstrating their potential clinical relevance for improving itraconazole bioavailability. The itraconazole–succinic acid cocrystals produced using CO_2 as an antisolvent have the fastest release profile, achieving 92% release in 2 h. The itraconazole–succinic acid cocrystals produced

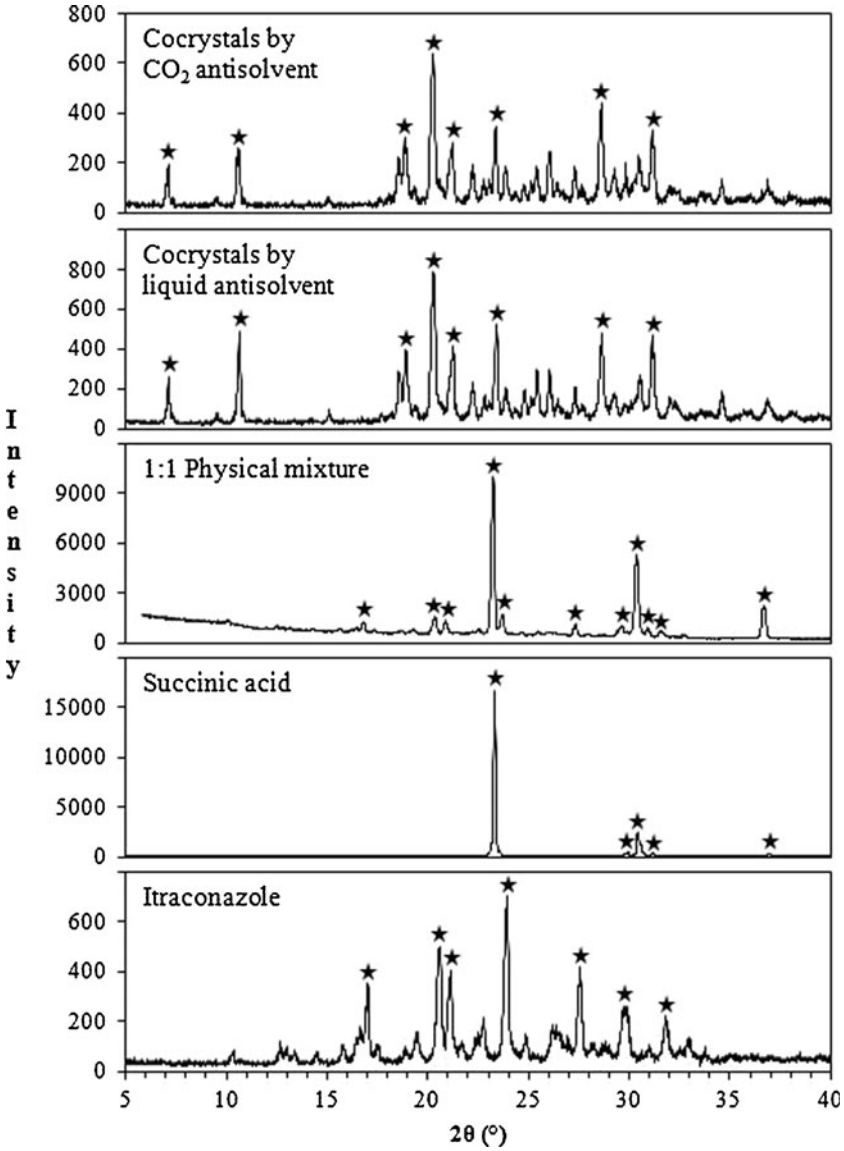

Fig. 2. PXRD patterns for itraconazole, succinic acid, a 1:1 by mass physical mixture of itraconazole and succinic acid, itraconazole–succinic acid cocrystals formed by liquid antisolvent, and itraconazole–succinic acid cocrystals formed by CO_2 antisolvent (*star* = characteristic peak)

using a liquid antisolvent have significantly slower release, achieving only 50% release in 2 h.

Cocrystal Stability

The dissolution benefits of a cocrystal are only realizable if the cocrystal structure is stable. Thermal stress is commonly used for accelerated stability studies, whereby correlation with an Arrhenius equation can predict the chemical and physical stability of a formulation during shelf storage at ambient conditions. For this study, the cocrystals were stored at 90°C with no humidity (dry) for 7, 14, and 28 days and changes in crystallinity assessed by PXRD. The effects of thermal stress on the crystallinity of the cocrystals produced by liquid and CO_2 antisolvent techniques are shown in Figs. 7 and 8, respectively. There were no new peaks, no peak shifts, and no polymorphic transformations observed in any of the samples. Most notably, the cocrystals produced by both methods maintained their structures and did not convert back to the free drug and former. Decreases in crystallinity, signified by decreases in peak intensity, were noticeable in all thermally treated samples, but there was not a definitive correlation between the duration of thermal exposure and the decrease in crystallinity. It is thought that an increase in thermal energy may cause some fraction of the cocrystal's hydrogen bonds to break, due to temperature-dependent proton disorder (34), leading to a less crystalline structure.

DISCUSSION

Cocrystal Formation by GAS Crystallization

Itraconazole and succinic acid both exhibit very low solubility in supercritical CO_2, making CO_2 antisolvent techniques

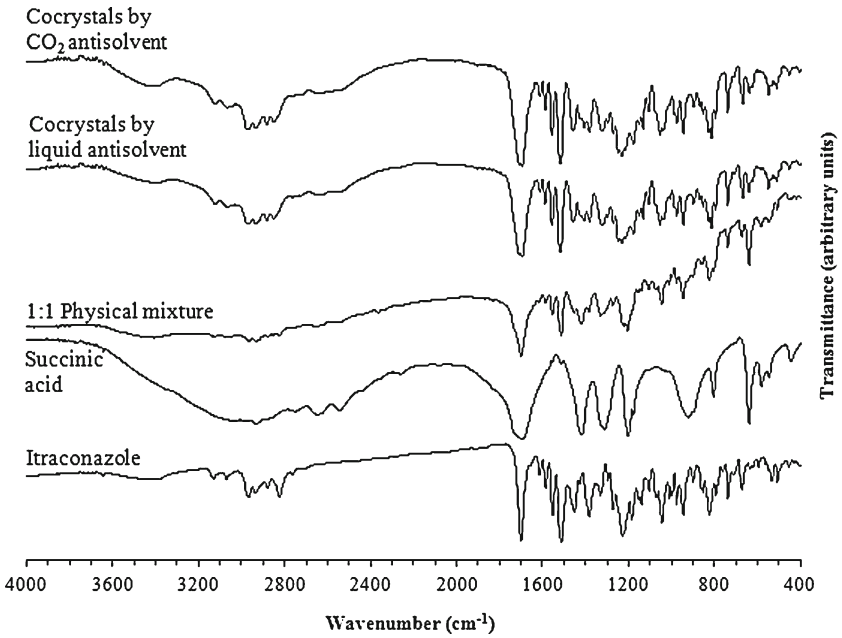

Fig. 3. FTIR spectra for itraconazole, succinic acid, a 1:1 by mass physical mixture of itraconazole and succinic acid, itraconazole–succinic acid cocrystals formed by liquid antisolvent, and itraconazole–succinic acid cocrystals formed by CO_2 antisolvent

ideal for their crystallization (35,36). The liquid solvent used in this work, THF, is a polar aprotic solvent capable of dissolving both itraconazole and succinic acid and previously shown to facilitate itraconazole–carboxylic acid cocrystal formation (37). Itraconazole has been reported to be sparingly soluble in THF, while succinic acid shows high solubility in the solvent (30,38). Cocrystallization using CO_2-expanded THF requires that itraconazole and succinic acid crystallize at similar and ideally stoichiometric rates. If the less soluble component, itraconazole, was to crystallize first, then cocrystallization would likely not occur. Since itraconazole and succinic acid solubility are complex functions of CO_2 pressure, solvent expansion, and cosolvent effects in a quaternary component system, the approach taken in this work was to prevent itraconazole recrystallization by providing a stoichiometric excess of succinic acid. A stoichiometric excess of former has been previously employed in the preparation of itraconazole–carboxylic acid cocrystals by liquid antisolvent and thermal crystallization techniques (39,40).

The proposed cocrystal structure for itraconazole and succinic acid involves the formation of two hydrogen bonds between the triazoles of two itraconazole molecules and the hydroxyl groups of a single succinic acid molecule. This hydrogen bonding scheme allows a single succinic acid molecule to tether two anti-parallel-oriented itraconazole molecules and thus fill a void space between the molecules, as shown in Fig. 9. Itraconazole and carboxylic acid cocrystals have been known to favor geometric fit over acid–base chemistry, which would predict interaction with the strongest base of itraconazole, piperazine (41). The starting quantities of itraconazole (250 mg) and succinic acid (100 mg) were provided in a stoichiometric ratio of 1:2.4 (itraconazole:succinic acid) despite the expected cocrystal stoichiometry of 2:1.

Table I. Vibrational Frequencies of Key Hydrogen Bonding Functional Groups

Functional group	Frequency (cm^{-1})			
	Itraconazole	Succinic acid	Cocrystals by liquid antisolvent	Cocrystals by CO_2 antisolvent
O–H stretch	–	2,650	2,630	2,630
C–N stretch	1,431	–	1,437	1,437
C=N stretch	1,614	–	1,610	1,612

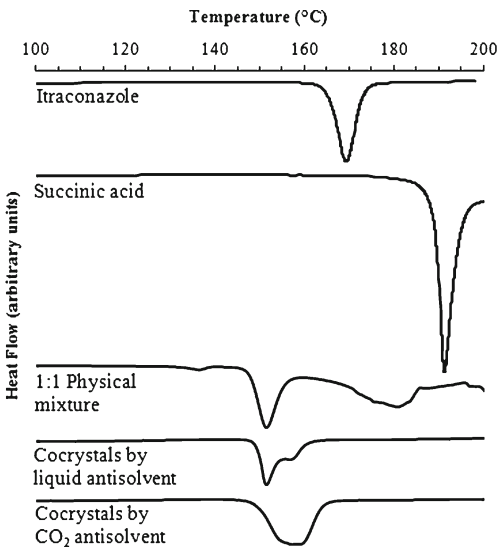

Fig. 4. DSC thermographs for itraconazole, succinic acid, a 1:1 by mass physical mixture of itraconazole and succinic acid, itraconazole–succinic acid cocrystals formed by liquid antisolvent, and itraconazole–succinic acid cocrystals formed by CO_2 antisolvent

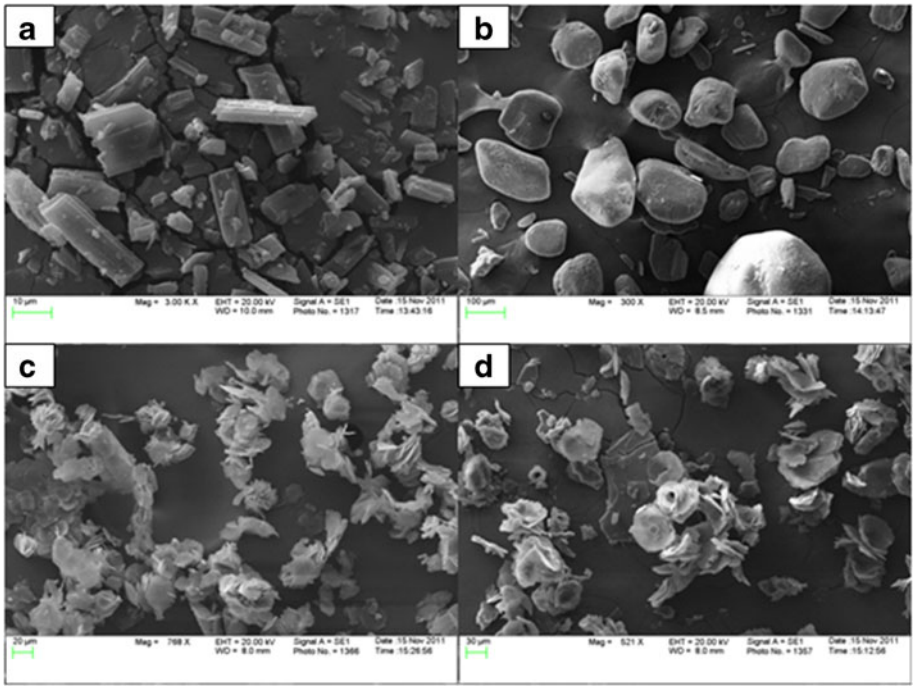

Fig. 5. SEM images of **a** itraconazole, **b** succinic acid, **c** itraconazole—succinic acid cocrystals formed by liquid antisolvent, and **d** itraconazole—succinic acid cocrystals formed by CO_2 antisolvent

Product yield is an important consideration in crystallization processes. Materials left behind in solution can inhibit solvent recycling and lead to increased costs, especially when working with expensive pharmaceutical compounds. By using excess succinic acid for cocrystal formation the amount of uncocrystallized itraconazole, the more expensive compound, can be minimized. For both methods of cocrystallization, liquid and CO_2 antisolvent, crystallization is dictated by supersaturation which is primarily a function of the concentration of material and choice of solvent and antisolvent. In practice, however, the yield is also affected by powder collection from the crystallization beaker or vessel, in which some crystallized material is inevitably left behind. In this work, the liquid antisolvent technique gave a product yield of 69.4% while the CO_2 antisolvent technique gave a product yield of 75.4%. It is expected that both of these yields would increase upon scale-up, where a smaller percentage of the crystallized material would be left behind.

Characterization of the Cocrystalline Phase

The PXRD patterns in Fig. 2 clearly demonstrate the formation of a new phase following simultaneous crystallization of itraconazole and succinic acid using either *n*-heptane or CO_2 as the antisolvent. Cocrystal formation was confirmed by the presence of characteristic itraconazole–succinic acid cocrystal peaks at 7.1°, 10.6°, 18.9°, 20.2°, 28.6°, and 31.1°, according to previous literature (29,42). The two additional crystalline peaks denoted in the cocrystal patterns correspond to two of the most intensely crystalline peaks of pure itraconazole (21.2°) and pure succinic acid (23.4°). A recent study showed that the intensity of characteristic cocrystal peaks could be used to quantitatively determine the amount of cocrystalline phase in a sample also containing the pure components (43). While quantitative PXRD analysis would be inappropriate without using identical masses of sample, the presence of pure component peaks in the cocrystal patterns

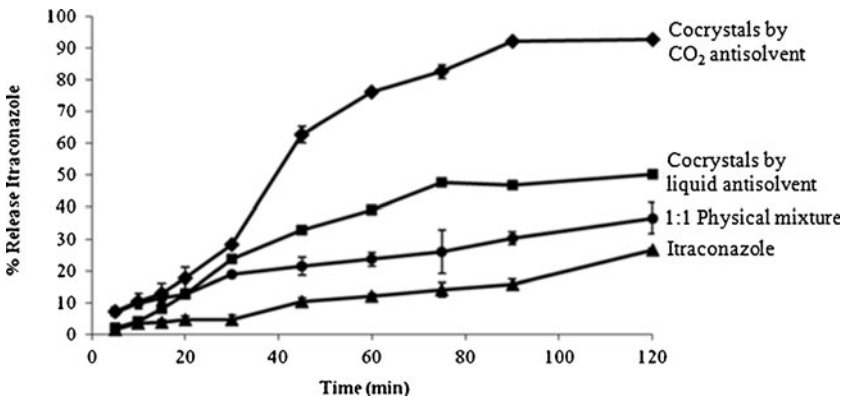

Fig. 6. Dissolution profiles for itraconazole, a 1:1 by mass physical mixture of itraconazole and succinic acid, itraconazole–succinic acid cocrystals formed by liquid antisolvent, and itraconazole–succinic acid cocrystals formed by CO_2 antisolvent

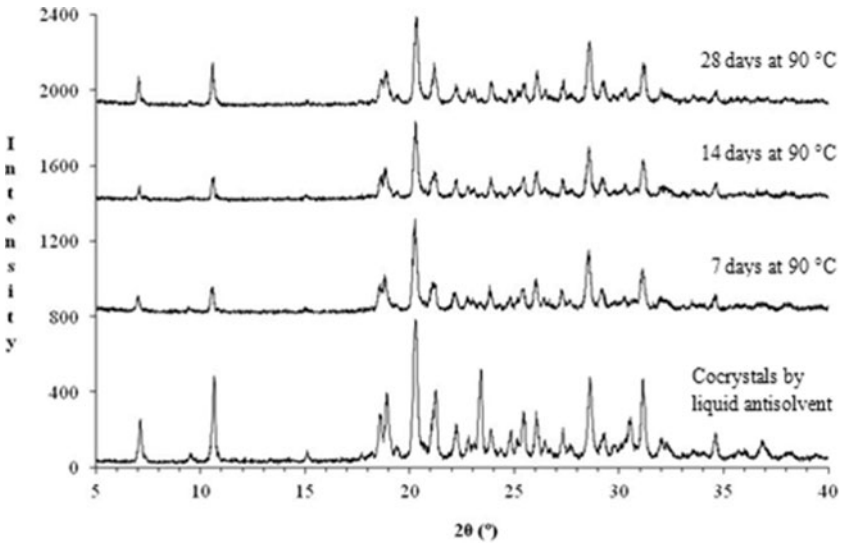

Fig. 7. PXRD spectra for itraconazole–succinic acid cocrystals formed by liquid antisolvent after 0, 7, 14, and 28 days at 90°C

indicate that there is likely uncocrystallized components in the final cocrystal products obtained in this work. The degree of crystallinity of the cocrystals, as indicated by peak intensity, was slightly less for the cocrystals crystallized using CO_2 compared to the liquid antisolvent. It is thought that the higher diffusivity of pressurized CO_2, as compared to *n*-heptane, promotes rapid mass transfer between the solvent and antisolvent phases which facilitates cocrystallization but inhibits crystal lattice organization.

Despite incomplete crystal lattice organization, it appears that the expected trimeric 2:1 itraconazole–succinic acid structure has been obtained using both cocrystal preparation techniques. The transition of the O–H stretch of succinic acid from 2,650 to 2,630 cm^{-1} suggests that this group is participating in a strong hydrogen bond in the cocrystal structure. A similar decrease was observed for the O–H stretching frequency of the carboxylic acid group of indomethacin which is thought to participate in hydrogen bonding with saccharin to form the indomethacin–saccharin cocrystal (44). Although the C–N and C=N groups of itraconazole are likely participating in a hydrogen bond with succinic acid, their vibrational frequencies are less affected by the interaction due to their aromatic impaired flexibility. For the itraconazole–succinic acid cocrystal, it appears that the use of compressed CO_2 has not resulted in the formation of any unique hydrogen bond interactions but has given the same cocrystal obtainable by a traditional liquid antisolvent technique.

The composition of the cocrystal powder produced by each method was determined by HPLC. The powder produced using the liquid antisolvent was found to contain 71.4% itraconazole by mass, or a 1:2.4 molar ratio of drug to former, while the powder produced using CO_2 as the antisolvent was found to contain 65.5% itraconazole by mass, or a 1:3.1 molar ratio. Considering that the cocrystal structure has a 2:1 itraconazole to succinic acid molar ratio, these ratios indicate the presence of excess uncocrystallized material in the final cocrystal powder. Without a reliable method to differentiate uncocrystallized itraconazole and succinic acid from

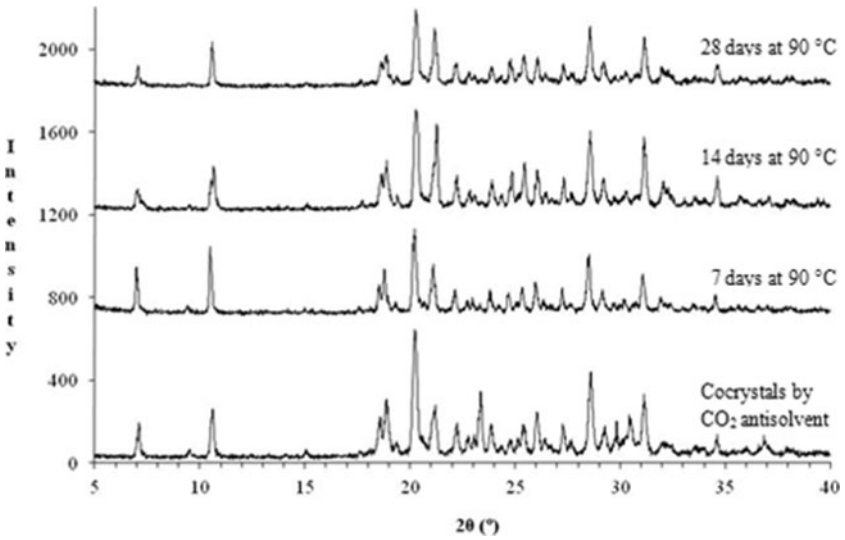

Fig. 8. PXRD spectra for itraconazole–succinic acid cocrystals formed by CO_2 antisolvent after 0, 7, 14, and 28 days at 90°C

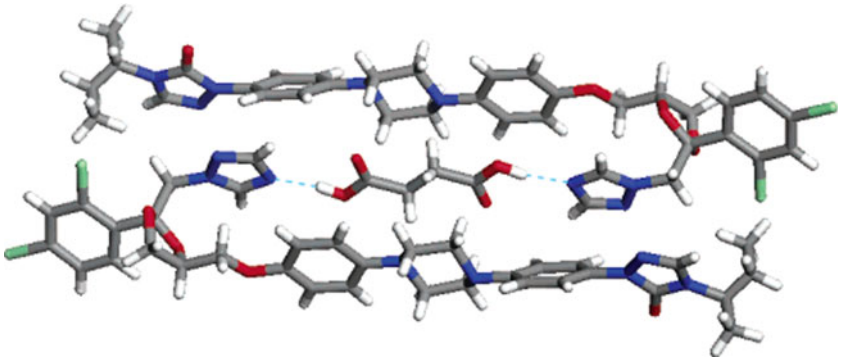

Fig. 9. Chemical structure of a 2:1 itraconazole–succinic acid cocrystal (29) (reproduced with permission from the American Chemical Society.)

cocrystallized, we cannot say with certainty based off these results which method, if either, leads to a greater fraction of cocrystals in the final product. It is thought, however, that the method of cocrystal preparation may play a role in determining the composition of the final cocrystal powder. For example, when using a liquid antisolvent technique unprecipitated components remain in solution and are discarded following centrifugation. When the liquid solvent is removed by flushing with supercritical CO_2, the remaining solvent becomes supersaturated with the unprecipitated component(s) causing either additional cocrystallization or possibly recrystallization of the pure drug and/or former which subsequently became part of the final cocrystal product. These differences in solvent removal also rationalize why higher yields may be achieved with the CO_2 antisolvent technique, and provide a basis for future studies examining the optimal amount of former to direct cocrystallization while maximizing cocrystal product purity in GAS cocrystallization. The RSD of the itraconazole content in the cocrystal powder produced using the liquid antisolvent was 2.7% while that of the powder produced using CO_2 was 4.9%. Both methods are capable of producing drug powders which conform to the FDA standard for drug content homogeneity, less than 6.0% RSD (45). The RSDs show that despite the likely presence of uncocrystallized materials in the final cocrystal powder, there are not significant regions of heterogeneity.

The use of DSC in characterizing a cocrystal is limited, especially for cocrystal systems whose two components form eutectic mixtures. *In situ* cocrystal formation during DSC heating has been reported for some organic physical mixtures of binary eutectic systems when they are heated beyond their eutectic melting point (10,23). From the physical mixture DSC curve, it was determined that a physical mixture of itraconazole and succinic acid does form a eutectic, melting at a lower temperature than either of the two pure components. Additional heating does not appear to produce a cocrystal, but the second broad endothermic event from 160°C to 195°C can possibly be attributed to the melting of excess succinic acid. Nearly identical thermal behavior has been observed for a physical mixture of urea and sulfamethazine which also forms a eutectic but does not cocrystallize upon heating (23). Itraconazole–succinic acid cocrystals have previously been reported to melt at 160.3°C (42). Therefore, it is suspected that the broad endothermic events between 145°C and 165°C for the cocrystals prepared by each method represent the eutectic melting of the residual uncocrystallized pure components followed by melting of the cocrystal. From the cocrystal DSC curves, it appears that GAS cocrystallization produces a cocrystal product with a qualitatively greater fraction of cocrystals, as the enthalpy of cocrystal melting was greater, compared to the liquid antisolvent technique. From these results it appears that during removal of the liquid solvent with supercritical CO_2, supersaturation may be promoting additional cocrystallization, and therefore maximizing the yield of cocrystals.

Dissolution Enhancement by GAS Cocrystallization

Despite the cocrystals produced by each method having similar crystal and chemical structures as determined by PXRD and FTIR, it appears that morphological and compositional differences resulting from the method of preparation can have a strong effect on drug dissolution. Both methods of cocrystal preparation gave thin flakes, a morphology previously observed in itraconazole crystallization (46). The flakes, characterized by a length, width, and height, cannot be sized by conventional means (light scattering) and determining a particle size distribution would have little value. Furthermore, since the particles are not submicron, particle size is not expected to have a significant influence on the dissolution rate. Based on a prior publication (46) in which the specific surface area of $\sim 20 \times 5 \times 1$ μm ($l \times w \times h$) itraconazole flakes was determined, it is expected that the cocrystal products produced by both methods would have nearly identical specific surface areas of ~ 2 m^2/g. Therefore, it is not expected that particle size or surface area is responsible for the enhanced dissolution of the itraconazole–succinic acid cocrystals produced by GAS cocrystallization.

While primary particle size and shape was similar for both methods of cocrystal preparation, agglomeration tendencies differed with respect to the antisolvent employed. The spherulite structures obtained during liquid antisolvent cocrystallization (Fig. 5c) were nearly identical to those obtained in the literature for antisolvent crystallization of theophylline (47). The formation of such agglomerates was attributed to the existence of two phases of solvent and antisolvent with crystallization occurring in discrete antisolvent droplets. It is suspected that the spherulite structures formed using the liquid antisolvent process actually inhibit itraconazole dissolution by blocking aqueous permeation to the center of the particle through the formation of a surface tension "skin" between adjacent radiating plates. The rosette structures observed when using CO_2 as an antisolvent (Fig. 5d) are thought to result from initial flake nucleation followed by subsequent

flake attachment. Rosettes have been known to possess improved flowability, a property critical for effective tabletting of pharmaceuticals, over other types of particle morphology such as needles (48). It also appears that the open central cavity of the rosette structures facilitates dissolution by allowing increased water permeation. These results suggest that cocrystal morphology, which can be altered by the method of preparation and within a preparation method (i.e., CO_2 antisolvent) by such factors as the pressure profile, can have a dramatic effect on drug dissolution.

The dissolution of itraconazole is pH dependent, especially around a pH of 1.0 due to itraconazole's second pK_a of ~1.5. While the amount of succinic acid used, ≤ 5 mg in 450 mL of dissolution medium, is not enough to affect the solution pH, the effect of uncocrystallized components on itraconazole dissolution is worth considering. From the DSC results, it was determined that the cocrystal product produced using the liquid antisolvent technique contained uncocrystallized itraconazole and succinic acid which underwent eutectic melting similar to the physical mixture. While eutectic melting also occurred for the cocrystal product formed by the CO_2 antisolvent technique, it was to a lesser extent likely due to lesser quantities of uncocrystallized components present. Therefore, it is suspected that the dissolution profile of the cocrystals produced by liquid antisolvent represents the dissolution of some cocrystallized itraconazole and some uncocrystallized itraconazole, while the dissolution profile for the cocrystals produced by CO_2 antisolvent represents the dissolution of itraconazole–succinic acid cocrystals with a significantly lesser amount of uncocrystallized itraconazole. Future studies will seek to quantify the amounts of cocrystallized and uncocrystallized itraconazole in a mixed product and work to maximize cocrystallization. Nonetheless, the dissolution rate enhancement of the itraconazole–succinic acid cocrystals produced by GAS cocrystallization is expected to be preserved during shelf storage due to maintenance of the cocrystal structure under thermal stress as shown in Fig. 8.

CONCLUSION

The feasibility of GAS cocrystallization for producing itraconazole–succinic acid cocrystals from THF was compared to a traditional liquid antisolvent process using *n*-heptane. Itraconazole–succinic acid cocrystals of similar crystallinity and chemical structure were produced by both methods. While PXRD and FTIR analysis support previous literature findings of a 2:1 itraconazole to succinic acid trimeric cocrystal structure formed by hydrogen bonding between the triazoles of two itraconazole molecules and the hydroxyl groups of a single succinic acid molecule, compositional analysis and DSC have revealed the presence of some fraction of uncocrystallized components which undergo eutectic melting when heated. The itraconazole–succinic acid cocrystals produced by both methods appear to have potential clinical relevance, with the cocrystals formed by GAS cocrystallization achieving over 90% dissolution in less than 2 h. Furthermore, the cocrystals appeared stable against dissociation under accelerated stability conditions for up to 4 weeks, suffering only moderate decreases in crystallinity thought to be attributed to the energetic breaking of some fraction of the cocrystal's hydrogen bonds. Through the preparation of itraconazole–succinic acid cocrystals, this work has shown the potential for inexpensive and environmentally benign CO_2 to replace traditional liquid antisolvents, offering advantages for cocrystal production scale-up.

ACKNOWLEDGMENT

The authors wish to acknowledge financial support from the National Science Foundation through NIRT grant DMI-0506722.

REFERENCES

1. Aakeröy CB, Forbes S, Desper J. Using cocrystals to systematically modulate aqueous solubility and melting behavior of an anticancer drug. J Am Chem Soc. 2009;131(47):17048–9.
2. Good DJ, Rodríguez-Hornedo N. Solubility advantage of pharmaceutical cocrystals. Cryst Growth Des. 2009;9(5):2252–64.
3. Trask AV, Motherwell WD, Jones W. Physical stability enhancement of theophylline via cocrystallization. Int J Pharm. 2006;320 (1):114–23.
4. Sun CC, Hou H. Improving mechanical properties of caffeine and methyl gallate crystals by cocrystallization. Cryst Growth Des. 2008;8(5):1575–9.
5. Karki S, Friščić T, Fábián L, Laity PR, Day GM, Jones W. Improving mechanical properties of crystalline solids by cocrystal formation: new compressible forms of paracetamol. Adv Mater. 2009;21(38–39):3905–9.
6. Morissette SL, Almarsson Ö, Peterson ML, Remenar JF, Read MJ, Lemmo AV, *et al*. High-throughput crystallization: polymorphs, salts, co-crystals and solvates of pharmaceutical solids. Adv Drug Deliv Rev. 2004;56(3):275–300.
7. Trask AV, Jones W. Crystal engineering of organic cocrystals by the solid-state grinding approach. Org Solid State React. 2005;41–70.
8. Horst JH, Cains PW. Co-crystal polymorphs from a solvent-mediated transformation. Cryst Growth Des. 2008;8(7):2537–42.
9. Qiao N, Li M, Schlindwein W, Malek N, Davies A, Trappitt G. Pharmaceutical cocrystals: an overview. Int J Pharm. 2011;419(1–2):1–11.
10. Padrela L, Rodrigues MA, Velaga SP, Matos HA, De Azevedo EG. Formation of indomethacin-saccharin cocrystals using supercritical fluid technology. Eur J Pharm Sci. 2009;38(1):9–17.
11. Padrela L, Rodrigues MA, Velaga SP, Fernandes AC, Matos HA, de Azevedo EG. Screening for pharmaceutical cocrystals using the supercritical fluid enhanced atomization process. J Supercrit Fluids. 2010;53(1–3):156–64.
12. Subramaniam B, Rajewski RA, Snavely K. Pharmaceutical processing with supercritical carbon dioxide. J Pharm Sci. 1997;86 (8):885–90.
13. Berends EM, Bruinsma OSL, De Graauw J, van Rosmalen GM. Crystallization of phenanthrene from toluene with carbon dioxide by the GAS process. AIChE J. 1996;42(2):431–9.
14. Kitamura M, Yamamoto M, Yoshinaga Y, Masuoka H. Crystal size control of sulfathiazole using high pressure carbon dioxide. J Cryst Growth. 1997;178(3):378–86.
15. Corrigan OI, Crean AM. Comparative physicochemical properties of hydrocortisone-PVP composites prepared using supercritical carbon dioxide by the GAS anti-solvent recrystallization process, by coprecipitation and by spray drying. Int J Pharm. 2002;245(1–2):75–82.
16. De Gioannis B, Jestin P, Subra P. Morphology and growth control of griseofulvin recrystallized by compressed carbon dioxide as antisolvent. J Cryst Growth. 2004;262(1–4):519–26.
17. Roy C, Vrel D, Vega-González A, Jestin P, Laugier S, Subra-Paternault P. Effect of CO2-antisolvent techniques on size distribution and crystal lattice of theophylline. J Supercrit Fluids. 2011;57:267–77.
18. Bertucco A, Lora M, Kikic I. Fractional crystallization by gas antisolvent technique: theory and experiments. AIChE J. 1998;44 (10):2149–58.

19. Elvassore N, Bertucco A, Caliceti P. Production of insulin-loaded poly (ethylene glycol)/poly (l-lactide)(PEG/PLA) nanoparticles by gas antisolvent techniques. J Pharm Sci. 2001;90(10):1628–36.
20. Park SJ, Yeo SD. Recrystallization of caffeine using gas antisolvent process. J Supercrit Fluids. 2008;47(1):85–92.
21. Shikhar A, Bommana MM, Gupta SS, Squillante E. Formulation development of Carbamazepine-Nicotinamide co-crystals complexed with γ-cyclodextrin using supercritical fluid process. J Supercrit Fluids. 2011;55(3):1070–8.
22. Ober CA, Montgomery SE, Gupta RB. Formation of itraconazole/L-malic acid cocrystals by gas antisolvent cocrystallization. Powder Technol. 2012(In press).
23. Lu E, Rodríguez-Hornedo N, Suryanarayanan R. A rapid thermal method for cocrystal screening. Cryst Eng Comm. 2008;10 (6):665–8.
24. Park SJ, Yeo SD. Recrystallization of phenylbutazone using supercritical fluid antisolvent process. Korean J Chem Eng. 2008;25 (3):575–80.
25. Rodrigues MA, Padrela L, Geraldes V, Santos J, Matos HA, Azevedo EG. Theophylline polymorphs by atomization of supercritical antisolvent induced suspensions. J Supercrit Fluids. 2011;58:303–12.
26. Yeo SD, Kim MS, Lee JC. Recrystallization of sulfathiazole and chlorpropamide using the supercritical fluid antisolvent process. J Supercrit Fluids. 2003;25(2):143–54.
27. Subra-Paternault P, Roy C, Vrel D, Vega-Gonzalez A, Domingo C. Solvent effect on tolbutamide crystallization induced by compressed CO2 as antisolvent. J Cryst Growth. 2007;309(1):76–85.
28. Bakhbakhi Y, Charpentier PA, Rohani S. Experimental study of the GAS process for producing microparticles of beclomethasone-17, 21-dipropionate suitable for pulmonary delivery. Int J Pharm. 2006;309(1):71–80.
29. Remenar JF, Morissette SL, Peterson ML, Moulton B, MacPhee JM, Guzman HR, *et al.* Crystal engineering of novel cocrystals of a triazole drug with 1, 4-dicarboxylic acids. J Am Chem Soc. 2003;125(28):8456–7.
30. Al-Badr AA, El-Subbagh HI. Itraconazole: comprehensive profile. Profiles Drug Subst Excip Relat Methodol. 2009;34:193–264.
31. Krishnan S, Raj CJ, Robert R, Ramanand A, Das SJ. Growth and characterization of succinic acid single crystals. Cryst Res Technol. 2007;42(11):1087–90.
32. Demiana IN. Formulation and evaluation of itraconazole via liquid crystal for topical delivery system. J Pharm Biomed Anal. 2001;26(3):387–99.
33. Krishnan S, Raj CJ, Priya SM, Robert R, Dinakaran S, Das SJ. Optical and dielectric studies on succinic acid single crystals. Cryst Res Technol. 2008;43(8):845–50.
34. Parkin A, Seaton CC, Blagden N, Wilson CC. Designing hydrogen bonds with temperature-dependent proton disorder: the effect of crystal environment. Cryst Growth Des. 2007;7(3):531–4.
35. Al Marzouqi AH, Shehatta I, Jobe B, Dowaidar A. Phase solubility and inclusion complex of itraconazole with cyclodextrin using supercritical carbon dioxide. J Pharm Sci. 2006;95(2):292–304.
36. Payne SM, Kerton FM. Solubility of bio-sourced feedstocks in 'green' solvents. Green Chem. 2010;12(9):1648–53.
37. Datta S, Grant DJW. Crystal structures of drugs: advances in determination, prediction and engineering. Nat Rev Drug Discov. 2004;3(1):42–57.
38. Schutz S, Wengatz I, Goodrow MH, Gee SJ, Hummel HE, Hammock BD. Development of an enzyme-linked immunosorbent assay for azadirachtins. J Agric Food Chem. 1997;45 (6):2363–8.
39. Remenar J, MacPhee M, Peterson ML, Morissette SL, Almarsson O. CIS-itraconazole crystalline forms and related processes, pharmaceutical compositions and methods. Google Patents. 2006.
40. Almarsson Ã, Hickey MB, Peterson ML, Zaworotko MJ, Moulton B, Rodriguez-Hornedo N. Pharmaceutical co-crystal compositions. Google Patents. 2011.
41. Morissette SL, Ãlmarsson AR, Peterson ML, Remenar JF, Read MJ, Lemmo AV, *et al.* High-throughput crystallization: polymorphs, salts, co-crystals and solvates of pharmaceutical solids. Adv Drug Deliv Rev. 2004;56(3):275–300.
42. Almarsson O, Hickey MB, Peterson ML, Zaworotko MJ, Moulton B, Rodriguez-Hornedo N. Pharmaceutical co-crystal compositions. US Patent 7,927,613; 2011.
43. Padrela L, de Azevedo EG, Velaga SP. Powder X-ray diffraction method for the quantification of cocrystals in the crystallization mixture. Drug Dev Ind Pharm. 2011;00:1–7.
44. Basavoju S, Bostrom D, Velaga SP. Indomethacin-saccharin cocrystal: design, synthesis and preliminary pharmaceutical characterization. Pharm Res. 2008;25(3):530–41.
45. Rohrs BR, Amidon GE, Meury RH, Secreast PJ, King HM, Skoug CJ. Particle size limits to meet USP content uniformity criteria for tablets and capsules. J Pharm Sci. 2006;95(5):1049–59.
46. Sathigari SK, Ober CA, Sanganwar GP, Gupta RB, Babu RJ. Single step preparation and deagglomeration of itraconazole microflakes by supercritical antisolvent method for dissolution enhancement. J Pharm Sci. 2011;100(7):2952–65.
47. Subra P, Laudani CG, Vega-Gonzalez A, Reverchon E. Precipitation and phase behavior of theophylline in solvent-supercritical CO2 mixtures. J Supercrit Fluids. 2005;35(2):95–105.
48. Booij J, Lefferts AG (inventors). Agglomerates by crystallization. 2005.